

Light Emission in the Unipolar Regime of Ambipolar Organic Field-Effect Transistors

W. S. Christian Roelofs,* Willem H. Adriaans, René A. J. Janssen, Martijn Kemerink, and Dago M. de Leeuw

Light emission from ambipolar organic field-effect transistors (OFETs) is often observed when they are operated in the unipolar regime. This is unexpected, the light emission should be completely suppressed, because in the unipolar regime only one type of charge carrier is accumulated. Here, an electroluminescent diketopyrrolopyrrole copolymer is investigated. Local potential measurements by scanning Kelvin probe microscopy reveal a recombination position that is unstable in time due to the presence of injection barriers. The electroluminescence and electrical transport have been numerically analyzed. It is shown that the counterintuitive unipolar light emission is quantitatively explained by injection of minority carriers into deep tail states of the semiconductor. The density of the injected minority carriers is small. Hence they are relatively immobile and they recombine close the contact with accumulated majority carriers. The unipolar light output is characterized by a constant efficiency independent of gate bias. It is argued that light emission from OFETs predominantly originates from the unipolar regime when the charge transport is injection limited.

1. Introduction

Light-emitting organic field-effect transistors (OFETs) are being investigated as a potential light source.^[1–3] For light emission holes and electrons need to recombine, hence both have to be present in the semiconductor. In the ambipolar regime both charges are accumulated simultaneously by biasing the gate in between the source and drain voltage. The charge carriers meet in the channel of the transistor, where electrons and holes recombine to form excitons and decay by the emission of light. The light output depends on the recombination rate which is proportional to the product of accumulated electron and hole density, on the singlet-triplet formation ratio, and on the photoluminescence efficiency of the semiconductor. The advantage of an OFET for light emission is the control of the recombination

zone. By choosing appropriate biases, this zone can be shifted away from the source and drain contacts.^[4–6] Quenching by the contacts is thereby avoided and high external quantum efficiencies have been reported.^[1] Recently developed electroluminescent ambipolar polymers with increasingly high and balanced electron and hole mobilities further enhance the opportunities for the use of OFETs as light sources.^[7]

The highest light output is expected when the transistor is operated in the bipolar regime, where the gate bias is in between the source and drain bias, such that simultaneously electrons are injected at the source contact and holes are injected from the drain contact (Figure 1c). Remarkably however, there are many examples in literature where electroluminescence is observed when the transistor is operated in one of the uni-

polar regimes (Figure 1d). In these examples a high light output has been obtained when the gate bias is not in between the source or the drain bias.^[4,8] Even light emission from entirely unipolar transistors has been reported.^[3,9,10] This is unexpected, the light emission should be completely suppressed in the unipolar regime, because then only one type of charge carrier is accumulated. No satisfactory explanation has been given for this peculiar light emission.

In our investigations on charge transport of diketopyrrolopyrrole-type polymers (DPP),^[11] we observed light emission from field-effect transistors. The highest electroluminescence intensity was obtained when the transistor was biased in the two unipolar regimes. In order to determine whether and where electrons and holes are present in the channel, we performed spatially resolved scanning Kelvin probe microscopy (SKPM) measurements. We show that the transistor behaves unstably in time when both electrons and holes are accumulated. Using device modeling we show that the instability is a result of the presence of injection barriers. As a consequence of the barrier, minority carriers cannot be injected into the transport level, but only in the tail of the density of states (DOS), which is present due to disorder in the semiconductor. We argue that the unipolar light emission is due to the recombination of the accumulated majority charge carriers with the minority carriers injected in the tail of the DOS at the contact.

W. S. C. Roelofs, W. H. Adriaans, Prof. R. A. J. Janssen, Dr. M. Kemerink
Eindhoven University of Technology
P.O. Box 513, 5600 MB Eindhoven, The Netherlands
E-mail: w.s.c.roelofs@tue.nl

Prof. D. M. de Leeuw
Max Planck Institute for Polymer Research
Ackermannweg 10, 55128 Mainz, Germany



DOI: 10.1002/adfm.201203568

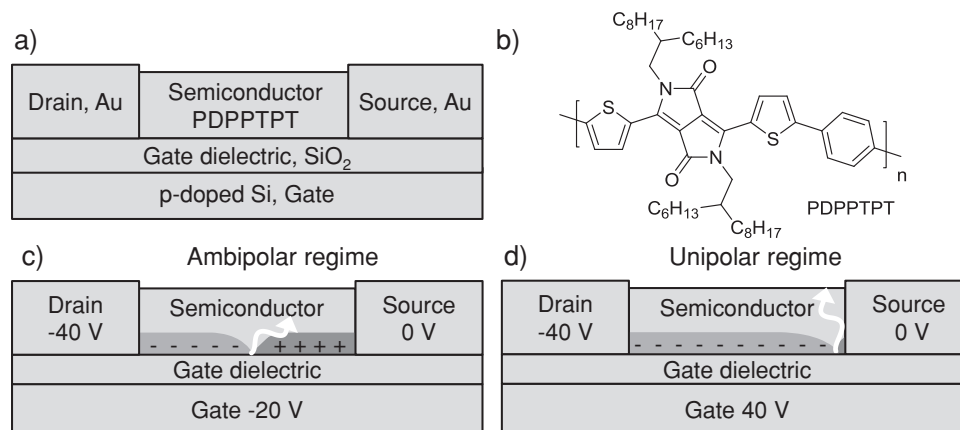


Figure 1. a) Schematic representation of the OFET used in this work. b) Chemical structure of PDPPTPT. c) Schematic of a transistor in the ambipolar regime. Light emission originates from the location where electrons and holes meet. d) Schematic of a transistor in the unipolar n-type regime. Light emission originates from the source, where the majority carriers are extracted.

2. Results and Discussion

2.1. Electrical and Optical Characterization

OFETs were fabricated on silicon substrates with gold source and drain electrodes and with poly[2,5-bis(2-hexyldecyl)-2,3,5,6-tetrahydro-3,6-dioxopyrrolo[3,4-c]pyrrole-1,4-diyl]-alt-([2,2'-(1,4-phenylene)bisthiophene]-5,5'-diyl)] (PDPPTPT, see Figure 1b for the chemical structure) as the semiconductor, as schematically presented in Figure 1a.^[12] Typical transfer curves

of the ambipolar OFETs are presented in Figure 2a. The gate bias was swept between -40 and 40 V and the drain bias was fixed at -20 , -40 , and -60 V. The transfer curves show ambipolar behavior; the current is enhanced at negative gate biases due to accumulation of holes and at positive gate biases due to accumulation of electrons. The extracted saturated electron and hole mobilities are around $0.02 \text{ cm}^2/\text{V s}$, similar to those obtained earlier.^[12] The mobilities extracted in the linear regime are strongly dependent on the gate bias due to disorder and due to the presence of injection barriers, especially for electrons. Mobilities extracted in the saturated regime at high gate biases

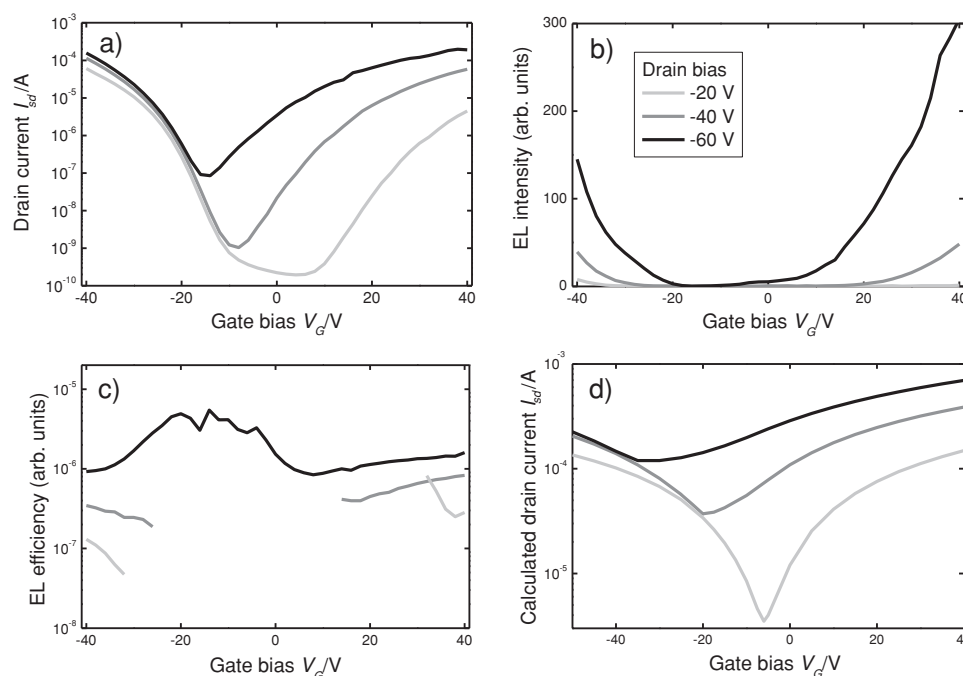


Figure 2. a) Transfer characteristics of an ambipolar organic transistor, measured at drain biases of -20 , -40 , and -60 V. b) The corresponding light emission of the transistor and c) the EL efficiency. d) Calculated transfer characteristics of a transistor with a constant mobility and an injection barrier for holes and electrons.

are only slightly underestimated.^[13] The presence of an energy barrier for injection is expected since the bandgap of PDPPTPT is around 1.5 eV and electrons and holes are both injected from gold electrodes. From the highest occupied molecular orbital (HOMO) and lowest unoccupied molecular orbital (LUMO) level energies as determined by cyclic voltammetry measurements^[12] and by using an estimated work function of gold of 4.7 eV, we arrive at a hole injection barrier of 0.7 eV and an electron injection barrier of 1.1 eV.^[14] The injection barriers are manifest in the output curves (shown in the Supporting Information) as an S-shaped curve at low drain bias.

The electroluminescence (EL) intensity probed by the photodiode increases with both the drain and the gate bias, presented in Figure 2b. The highest light output is obtained in the two extreme unipolar regimes. This implies that the recombination zone is located either at the source or the drain contact. The detected EL intensity is divided by the source-drain current to obtain a measure for the EL efficiency. This efficiency is presented in Figure 2c as a function of gate bias. The EL efficiency is low due to the low photoluminescence efficiency of the semiconductor. At drain biases of −20 and −40 V, the electroluminescence efficiency at low gate bias cannot be determined, because the light output is below the detection limit of the photodiode used. At higher gate biases the efficiency does not depend on the gate bias. Similarly, at a drain bias of −60 V the EL efficiency is constant for all gate biases. We note that a constant efficiency is not expected for a bipolar light emitting transistor. The efficiency should actually peak when the gate bias is halfway the source and drain bias and the recombination zone is in the middle of the channel, as experimentally verified.^[6] The constant EL efficiency is characteristic for a unipolar light emitting transistor; its origin will be elucidated below.

2.2. Local Channel Potential

To determine the location of the recombination zone we probed the local channel potential, $V(x)$, in the channel with SKPM, with x the position in the channel. We define the effective gate potential, V_{eff} , in the channel as the gate bias, V_G , with respect to the local surface potential, i.e., $V_{\text{eff}} = V_G - V(x)$. The locally accumulated surface charge density ρ is equal to the product of the effective gate bias and the gate capacitance, $\rho = -C_g V_{\text{eff}}$. Electrons are induced in the channel for a positive effective gate potential and holes are induced for a negative effective gate potential. At the recombination zone, the position where the charges recombine, there is no net accumulated charge and consequently the effective gate potential is zero. The measured channel potentials for fixed gate biases are presented in Figure 3a, with the drain bias set at +14 V. We first discuss the black line which is measured for a gate bias of 10 V. At small x , close to the drain electrode, the channel potential is larger than the applied gate potential. The effective gate potential is negative, which implies that holes are accumulated. The effective gate potential is zero at about $x = 5 \mu\text{m}$, so the recombination zone is close to the source contact, and predominantly holes are accumulated in the channel. The dark gray curve represents the surface potential measured at an only slightly higher gate bias of 10.5 V. The effective gate potential is now zero at about $x = 0.8 \mu\text{m}$, which

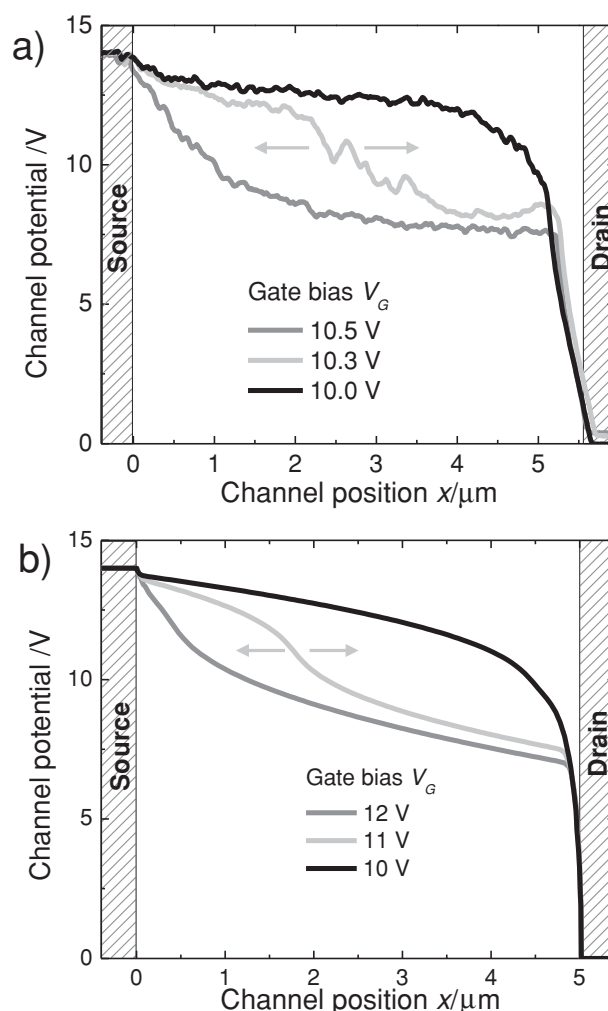


Figure 3. a) Measured surface potential in the channel of an operating ambipolar OFET. The gate of the transistor is biased in the ambipolar regime. At a gate bias of 10 V (black line) the effective gate potential is mainly positive, while at 10.5 V (dark gray line) the effective gate potential is mainly negative. The line in between in light gray is not time-stable. b) Simulated potential in an ambipolar transistor with a 0.39 eV injection barrier for holes and a 0.58 eV injection barrier for electrons. The arrows indicate the instability of the recombination zone.

implies that the recombination zone is now located close to the drain contact. Now predominantly electrons are accumulated in the channel. The light gray line represents a single measurement at an intermediate gate bias. However, the measurement is unstable; the recombination zone cannot reliably be determined. The position varies in time and oscillates between the two extremes. It is remarkable that the transistor switches from an almost unipolar electron channel to an almost unipolar hole channel when changing the applied gate bias by only 0.5 V.

We note that in all cases a voltage drop is observed at the contacts, which indicates the presence of a large injection barrier.^[15] The largest voltage drop or the biggest barrier is observed at the source where electrons are injected, in agreement with the estimation from the energy levels.

2.3. Drift-Diffusion Calculations

To explain the origin of the instability of the recombination zone, drift diffusion calculations were performed. The electrical transport model is based on the coupled drift-diffusion, Poisson, and current continuity equations that are numerically solved on a 2D rectangular grid. A density dependent mobility will decrease the conductivity of the minority channel in the transistor with respect to the majority channel, which destabilizes the recombination position. In order to disentangle the effect of injection barriers from effects due to a field- and density dependent mobility we use a constant mobility in the simulations. We note however that this approximation does not affect the generality of the conclusions. The charge injection is described by classical thermionic emission. The Emtage O'Dwyer model is used to take lowering of the injection barrier by the image force into account.^[16] This makes the charge injection field dependent. Electrons and holes are assumed to recombine via the Langevin mechanism. No loss mechanisms as exciton quenching are incorporated. The calculation method is described in detail in the supporting information.

As a first step we calculated the electrical transport. The transfer curves obtained are presented in Figure 2d. As input parameters we used the experimentally extracted saturated mobilities and an injection barrier for holes and electrons of 0.39 eV and 0.58 eV, respectively. We note that these values are lower than estimated above, since disorder lowers the effective injection barriers.^[16] The simulated results qualitatively agree with the measured transfer curves of Figure 2a. At high positive and negative gate biases, in the unipolar regimes, the absolute current values are dominated by the saturated mobility of 0.02 cm²/V s, which is used as input in the calculations. In the ambipolar regime, where the drain bias is larger than the gate bias, the calculated current is higher than the measured current. The origin is that we use a constant mobility in the calculations while the mobility is actually gate bias dependent.

It may seem counterintuitive that despite a large injection barrier charges can be injected, but in fact a field-effect transistor is tolerant for injection barriers. The origin is image-force lowering of the barrier due to the high electric field at the injecting contact. In a transistor under accumulation the electric field at the injecting contact progressively increases with increasing gate bias.^[17] Hence, at low gate bias the current is injection limited, but by increasing the gate bias injection barriers up to 1 eV can be surmounted.^[17]

2.4. Unstable Recombination Position

The calculated surface potentials as a function of gate bias are presented in Figure 3b. We used the same input parameters as used for the calculation of the transfer curves, viz. the extracted saturated mobilities and an injection barrier for holes of 0.39 eV and for electrons of 0.58 eV. Comparison of Figures 3a and Figure 3b shows that a good qualitative agreement between measured and calculated potentials is obtained. The black line represents an almost unipolar p-type channel and the dark gray curve an almost unipolar n-type channel. The position of the recombination zone close to either the source or the drain

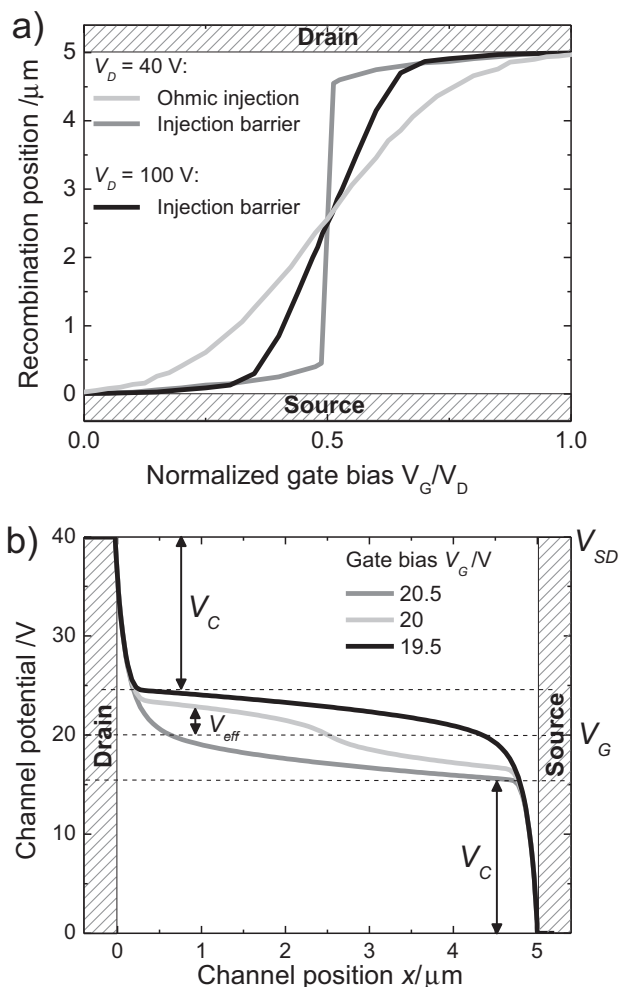


Figure 4. a) The position where recombination takes place in an ambipolar OFET as function of the gate bias normalized by the drain voltage for three situations. In dark gray the situation as in figure 2b with injection barriers of 0.65 eV for both holes and electrons and 40 V at the drain, in black the situation with identical injection barriers and 100 V at the drain, and in light gray the situation with Ohmic injection. b) The potential in the channel of an OFET with injection barriers of 0.65 eV for both holes and electrons and 40 V at the drain for three different gate biases. The effective gate potential, V_{eff} , in the channel is reduced due to the voltage drop at the contacts.

contact is reproduced. Within a bias window of 2 V the transistor operation switches from unipolar hole to unipolar electron transport. For intermediate gate biases the position of the recombination zone strongly depends on the input parameters. Note that the heights of the barriers are chosen such that the calculated potential drop in Figure 3b corresponds with the measured potential drop in Figure 3a. The exact values of the injection barriers are not critical for the behavior of the transistor as will be explained below. If the barriers are increased to, for example, 0.65 eV the same unstable behavior is observed, as shown in Figure 4b.

The experimentally and numerically established extreme sensitivity of the recombination zone position on gate bias can be understood as follows. We distinguish three regions in the

transistor, two interfacial regions near the contacts and one bulk region in between. The total applied source-drain bias V_{SD} is distributed over these three regions. In absence of injection barriers V_{SD} entirely drops over the bulk region. In this situation, the recombination zone position can be gradually moved across the bulk region by varying the effective gate bias between 0 and V_{SD} . The position of the recombination zone as function of gate bias calculated without injection barriers is presented with the light gray line in Figure 4a. Note that we so far tacitly assumed identical source and drain contacts which, in combination with zero hole and electron injection barriers (Ohmic contacts), implies a zero bandgap semiconductor. For a semiconductor with a finite bandgap E_g , significant ambipolar transport only sets in when $V_{SD} > E_g$. Assuming a symmetric device, the recombination zone position moves across the bulk region when the effective gate bias is between $E_g/2$ and $V_{SD} - E_g/2$. We now drop the Ohmic contact assumption. Part of the source-drain bias, V_C , will now fall across the interfacial region at both the source and the drain. Then only $V_{SD} - 2V_C$ will fall over the bulk region. An example of such a situation is depicted in Figure 4b where 0.65 eV injection barriers are used for both holes and electrons. The recombination zone position moves across the bulk region for effective gate biases between $V_C + E_g/2$ and $V_{SD} - V_C - E_g/2$, still assuming symmetry. This condition can be understood by regarding the bulk region as a separate ambipolar channel with Ohmic contacts, albeit with a lower applied source-drain bias of $V_{SD} - V_C$. Hence, it is clear that with increasing importance of injection barriers (increasing V_C) the sensitivity of the recombination zone position on gate bias increases, i.e., it runs from one side of the bulk to the other in an increasingly narrow window of the effective gate voltage, c.f. the black and dark gray lines in Figure 4a. The ultimate situation is reached when the device is fully injection limited. In that case, ambipolarity still demands both electron and hole accumulation on either side of the recombination zone, so the voltage drop over the bulk must at least remain equal to, roughly, E_g , so $V_C = V_{SD} - E_g$. In this limit, the gate voltage window in which the recombination zone transits the entire bulk region goes to zero: any small change affecting the electrostatics in the device may completely shift the recombination zone. The recombination zone is unstable.

2.5. Description of Unipolar Light Emission

The light output is proportional to the recombination current. Hence we calculated the recombination current as a function of gate bias, with similar input parameters used for the simulation of Figure 2a and Figure 3b, viz. a constant mobility. Irrespective of the injection barrier, the highest light output is obtained in the ambipolar regime, when the gate bias is about in between the source and drain bias. The light output decreases with increasing gate bias. In the limiting case of the unipolar regime when the gate bias is close to either the source and drain bias the light output is negligible. The experimental data of Figure 2b cannot be reproduced; the reason being that the density of minority carriers in the calculations is too low. The explanation is elucidated in **Figure 5**. A transistor is biased in the unipolar p-type regime. Holes are injected by the drain

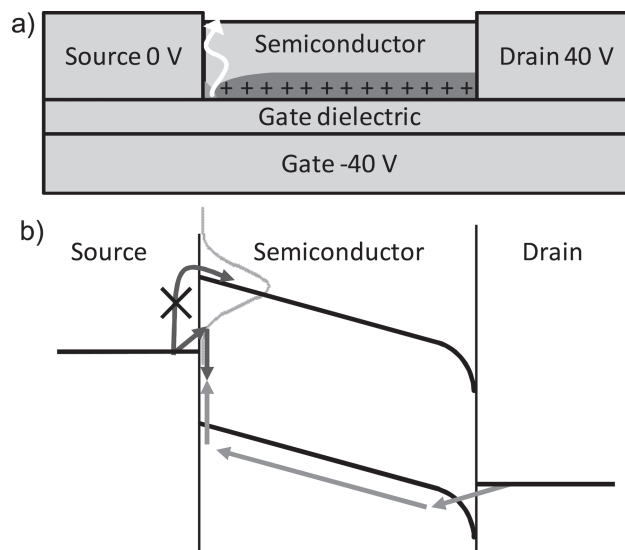


Figure 5. a) Schematic of an OFET biased in the unipolar p-type regime. b) Schematic of the corresponding band diagram. The Gaussian depicts the broadened density of states. The dark gray arrows represent the movement of holes and the light gray arrows the movement of electrons. The injection barrier is too high for the minority carriers, the electrons, to be injected in mobile states.

and accumulated in the channel. The band diagram shows an injection barrier. Due to the accumulated holes in the channel, a large fraction of the source-drain bias drops near the drain contact. The resulting high electric field leads to strong image forces, effectively eliminating the injection barrier for holes. This mechanism does not apply for the minority carriers, here electrons from the source. Since the gate does not accumulate electrons there is no significant electric field near the source, hence no image force barrier lowering. In the calculations electrons have to overcome an insurmountable energy barrier and the density of injected electrons is negligible. Consequently there is no recombination.

To explain the experimentally observed light output the injection mechanism has to be adapted. So far we have assumed injection into a single transport level with a well defined energy. For semiconducting polymers the energy bands are broadened by disorder. As illustrated in Figure 5, minority carriers can be injected into the tail states that are lower in energy. Both the density and the mobility of the tail states is low.^[18] The current is therefore still dominated by the majority carriers; the minority carrier current density can be disregarded. The calculations are adjusted by introducing a low density of tail states at a lower energy than the mobile states. Transport between tail states only occurs by thermal activation via the mobile states. We note that the outcome of the calculations is independent of the mobility of the tail states, as long as the density and mobility of the tail states is significantly lower than the states higher in energy.

The adapted description of minority carrier injection does not affect the results of Figure 2d and Figure 3b. In the ambipolar regime minority carriers do not play a role for charge transport and its density is low. The calculated electroluminescence intensity, which is proportional to the recombination

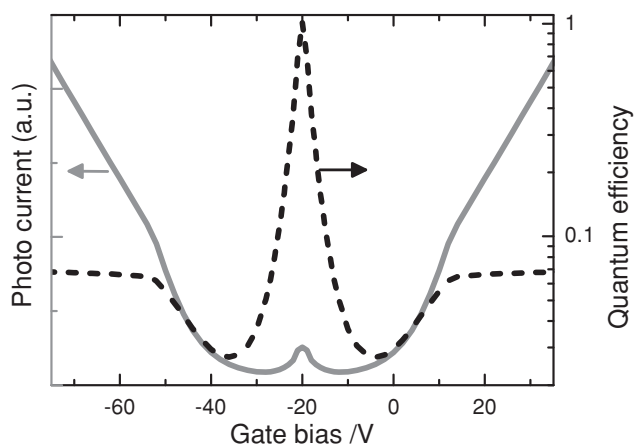


Figure 6. Solid line (left axis): the calculated EL intensity as function of gate bias when injection in tail states is incorporated in the simulation. Dashed line (right axis): the corresponding efficiency. The drain bias was set at 40 V.

current, is presented in **Figure 6** as a function of gate bias. The highest light output is obtained in the two extreme unipolar regimes, when the gate bias is close to either the source or the drain potential. A good qualitative agreement with the experimental data of Figure 2b is obtained. The quantum efficiency, calculated by dividing the total recombination current by the source-drain current, is presented as the dashed line in Figure 6. In the unipolar regimes the efficiency is constant. The reason is that the efficiency only depends on the density of minority carriers, which does not change with gate bias. Quenching at the contacts, outcoupling and photoluminescence efficiencies are being ignored. The absolute value of the minority density depends on the local field at the majority extracting contact, the energy levels and density of the tail states. Effectively, the calculated efficiency strongly depends on the magnitude of the injection barrier. Figure 6 shows that the efficiency has a maximum in the ambipolar regime. However, the source-drain current is then low, and the electroluminescence intensity is much smaller than the unipolar light output. In the measurements the source-drain current is even lower in the ambipolar regime due to the density dependent mobility and, therefore, the peak is not observed. We note that a different injection mechanism for minority carriers has been reported by Santato et al.^[10] They need a potential drop at the minority carrier injecting contact. As explained above, this is highly unlikely.

3. Conclusions

The light emission in organic ambipolar field-effect transistors is investigated. SKPM measurements have shown that the recombination zone is unstable in the ambipolar regime. Numerical calculations have shown that this instability is a direct consequence of the presence of injection barriers. The highest light output is observed when the transistor is biased in the unipolar regime, where just one type of charge carrier is accumulated. This counterintuitive light emission is

quantitatively explained by taking injection of minority carriers into tail states into account. This injection starts to dominate when substantial injection barriers are present. The density of the injected minority carriers is small. Hence they are relatively immobile and they recombine close the contact with accumulated majority carriers. Field-effect transistors based on luminescent ambipolar semiconductors emit in the ambipolar regime when the contacts are Ohmic. However, when the charge transport is injection limited, unipolar light emission is obtained.

4. Experimental Section

Field-effect transistors were prepared on heavily doped Si wafers acting as common gate, with thermally grown SiO₂ as gate dielectric and lithographically patterned gold electrodes with a 2 nm Ti adhesion layer. The resulting finger transistors have a channel length and width of 10 μm and 1 cm, respectively, and a gate capacitance of $C_g = 17 \text{ nF/cm}^2$. To reduce gate bias stress, the gate dielectric was passivated with vapor deposited hexamethyldisilazane (HMDS). The organic semiconductor PDPPTPT was applied by spincoating from chloroform and annealed at 150 °C in vacuum for 24 h. The chemical structure of PDPPTPT is presented in Figure 1b. Transfer characteristics of the OFETs were measured in a high-vacuum (10^{-6} mbar) probe station with a Keithley 4200 source-measure unit. Light emission was probed by a Si photodiode (Siemens SFH 206 K) placed directly above the sample and connected to the Keithley 4200 and the EL efficiencies were derived by dividing the detected EL intensity by the source-drain current. Non-contact atomic force microscopy (AFM) and SKPM measurements were performed with an Omicron VT-SPM connected to a Nanonis controller in ultrahigh vacuum (10^{-9} mbar). Pt-Ir coated AFM-tips (PPP-EFM, Nanosensors, $f_{res} \approx 70 \text{ kHz}$) were used. For SKPM a 1 V AC-tip voltage ($\approx 650 \text{ Hz}$) was applied during scanning.

Supporting Information

Supporting Information is available from the Wiley Online Library or from the author.

Acknowledgements

The authors thank J. C. Bijleveld for the synthesis of the semiconductor PDPPTPT, Philips Research and MiPlaza for technical support and P. W. M. Blom for stimulating discussions. The authors gratefully acknowledge financial support from NanoNextNL, project 06D.03.

Received: December 3, 2012

Revised: February 4, 2013

Published online: March 26, 2013

- [1] R. Capelli, S. Toffanin, G. Generali, H. Usta, A. Facchetti, M. Muccini, *Nat. Mater.* **2010**, 9, 496.
- [2] a) M. C. Gwinner, D. Kabra, M. Roberts, T. J. K. Brenner, B. H. Wallikewitz, C. R. McNeill, R. H. Friend, H. Sirringhaus, *Adv. Mater.* **2012**, 24, 2728; b) T. Yamao, Y. Shimizu, K. Terasaki, S. Hotta, *Adv. Mater.* **2008**, 20, 4109.
- [3] A. Hepp, H. Heil, W. Weise, M. Ahles, R. Schmechel, H. von Seggern, *Phys. Rev. Lett.* **2003**, 91, 157406.
- [4] L. Bürgi, M. Turbiez, R. Pfeiffer, F. Bienewald, H.-J. Kirner, C. Winnewisser, *Adv. Mater.* **2008**, 20, 2217.

- [5] a) B. B. Y. Hsu, C. Duan, E. B. Namdas, A. Gutacker, J. D. Yuen, F. Huang, Y. Cao, G. C. Bazan, I. D. W. Samuel, A. J. Heeger, *Adv. Mater.* **2012**, *24*, 1171; b) J. Zaumseil, R. Friend, H. Sirringhaus, *Nat. Mater.* **2006**, *5*, 69.
- [6] E. C. P. Smits, S. Setayesh, T. D. Anthopoulos, M. Buechel, W. Nijssen, R. Coehoorn, P. W. M. Blom, B. de Boer, D. M. de Leeuw, *Adv. Mater.* **2007**, *19*, 734.
- [7] a) Z. Chen, M. J. Lee, R. Shahid Ashraf, Y. Gu, S. Albert-Seifried, M. Meedom Nielsen, B. Schroeder, T. D. Anthopoulos, M. Heeney, I. McCulloch, H. Sirringhaus, *Adv. Mater.* **2012**, *24*, 647; b) C. B. Nielsen, M. Turbiez, I. McCulloch, *Adv. Mater.* **2012**, DOI: 10.1002/adma.201201795; c) J. D. Yuen, J. Fan, J. Seifter, B. Lim, R. Hufschmid, A. J. Heeger, F. Wudl, *J. Am. Chem. Soc.* **2011**, *133*, 20799.
- [8] a) M. Ahles, A. Hepp, R. Schmechel, H. von Seggern, *Appl. Phys. Lett.* **2004**, *84*, 428; b) S. Jung Hwa, B. N. Ebinazar, G. Andrea, J. H. Alan, C. B. Guillermo, *Adv. Funct. Mater.* **2011**, *21*; c) J. H. Seo, E. B. Namdas, A. Gutacker, A. J. Heeger, G. C. Bazan, *Adv. Funct. Mater.* **2011**, *21*, 3667.
- [9] a) T. Sakanoue, E. Fujiwara, R. Yamada, H. Tada, *Appl. Phys. Lett.* **2004**, *84*, 3037; b) J. Zaumseil, H. Sirringhaus, *Chem. Rev.* **2007**, *107*, 1296.
- [10] C. Santato, R. Capelli, M. A. Loi, M. Murgia, F. Cicoira, V. A. L. Roy, P. Stallinga, R. Zamboni, C. Rost, S. F. Karg, M. Muccini, *Synth. Met.* **2004**, *146*, 329.
- [11] W. S. C. Roelofs, S. G. J. Mathijssen, J. C. Bijleveld, D. Raiteri, T. C. T. Geuns, M. Kemerink, E. Cantatore, R. A. J. Janssen, D. M. de Leeuw, *Appl. Phys. Lett.* **2011**, *98*, 203301.
- [12] J. C. Bijleveld, V. S. Gevaerts, D. Di Nuzzo, M. Turbiez, S. G. J. Mathijssen, D. M. de Leeuw, M. M. Wienk, R. A. J. Janssen, *Adv. Mater.* **2010**, *22*, E242.
- [13] L. Giraudet, O. Simonetti, *Org. Electron.* **2011**, *12*, 219.
- [14] X. Cheng, Y.-Y. Noh, J. Wang, M. Tello, J. Frisch, R.-P. Blum, A. Vollmer, J. P. Rabe, N. Koch, H. Sirringhaus, *Adv. Funct. Mater.* **2009**, *19*, 2407.
- [15] L. Burgi, H. Sirringhaus, R. H. Friend, *Appl. Phys. Lett.* **2002**, *80*, 2913.
- [16] J. J. M. van der Holst, M. A. Uijtewaal, B. Ramachandran, R. Coehoorn, P. A. Bobbert, G. A. de Wijs, R. A. de Groot, *Phys. Rev. B* **2009**, *79*, 85203.
- [17] J. J. Brondijk, F. Torricelli, E. C. P. Smits, P. W. M. Blom, D. M. de Leeuw, *Org. Electron.* **2012**, *13*, 1526.
- [18] C. Tanase, E. J. Meijer, P. W. M. Blom, D. M. de Leeuw, *Phys. Rev. Lett.* **2003**, *91*, 216601.